HIGHLIGHT

Check for updates

Coordination polymers with embedded recognition sites: lessons from cyclotriveratrylene-type ligands†

Matthew P. Snelgrove (iD) and Michaele J. Hardie (iD) *

A review of coordination polymers formed using multi-topic cyclotriveratrylene-type ligands. Cyclotriveratrylene (CTV) is a molecular host with a bowl-shaped tribenzo[*a,d,g*]cyclononatriene scaffold. Tripodal and hexapodal ligands with N-donor and O-donor groups have been developed and these form a range of coordination chains, 2D and 3D coordination networks with transition metals. Such ligands are molecular hosts so there is potential to form materials with both host-specific and lattice guest-binding sites. This highlight article will discuss how the host–guest properties of the ligands can compromise the ability of CTV-type ligands to form such materials as intracavity guest binding, bowl-in-bowl stacking and hand-shake inclusion motifs effectively block the host-specific binding site. A range of coordination polymer materials which do feature hierarchical guest-binding sites are formed from CTV-type ligands, most commonly where there are networks of coordination capsules or cage, or where alternating bowl-up, bowl-down arrangements of ligands within networks leads to tubular structures.

1. Introduction

Coordination polymers (CPs) and metal–organic frameworks (MOFs) are a class of crystalline materials with well-ordered framework structures composed of metal centres linked by organic bridging ligands.[1] Potential applications for such materials are wide-ranging and include catalysis, separations and extractions, medicinal applications, sensors, energy materials and gas storage.[2] MOFs and some coordination polymers are porous with robust channels and cavities that withstand post-construction removal of solvent molecules. A number of the applications for coordination polymers and MOFs are dependent on their ability to bind or host other molecular or ionic species within these pore-spaces. Robustness is not absolutely crucial to function, and crystalline-sponge materials can act as heterogeneous hosts provided guest solvent molecules can be exchanged without substantial loss of framework structure.[3] The ability of MOFs and some coordination polymers to bind guest molecules is a function of the overall assembly; the individual components that comprise the materials are not usually capable of this. Molecular hosts are a class of compounds where individual molecules are able to bind guest species through non-covalent interactions. The

construction of CP or MOF materials using molecular hosts as bridging ligands is therefore of interest as it has the potential to produce materials where there are both site-specific guest-binding pockets of the molecular host, alongside the lattice pore sites more typical of MOFs and porous coordination polymers. Thus, they may form hierarchical guest spaces capable of simultaneous binding of different guests, or ordered molecular recognition of guests, as also stated by Bew *et al.*: "formation of MOFs with calix[4]arene-based ligands opens up the possibility of forming hierarchically-porous materials, with two levels of porosity associated with both the ligand and the structural framework".[4]

There are many different types of molecular hosts which are generally macrocyclic and feature a molecular cavity of some type as a guest-binding site, a variety of molecular host have been employed as bridging ligands for MOFs and coordination polymers.[4–8] The most commonly thus utilised macrocycles are calixarenes and related cone-shaped hosts. Pillararenes, crown ethers, cucurbiturils and cyclodextrins have also been employed. Our own work,[9–21] alongside that of other research groups,[22–26] has investigated the use of functionalised cyclotriveratrylenes (CTVs) as bridging ligands for coordination polymers. Cyclotriveratrylene (CTV) is a bowl-shaped molecular host with a tribenzo[*a,d,g*] cyclononatriene core.[27] It has a pyramidal shape with an open upper-rim. Other common members of the CTV family include the tris-catechol cyclotricatechylene (CTC), and cyclotriguaiacylene (CTG), Chart 1. CTV-analogues with other functional groups appended to the upper rim are most

School of Chemistry, University of Leeds, Woodhouse Lane, Leeds LS2 9JT, UK.
E-mail: m.j.hardie@leeds.ac.uk

Chart 1 Members of the CTV family of molecular hosts.

commonly accessed through functionalisation of CTG to give tripodal analogues, or of CTC to give hexapodal analogues. The tripodal C_3-symmetric CTG-analogues are chiral with M and P isomers which undergo slow exchange via a saddle-conformation. Appending metal-binding ligand groups to the upper rim of CTG, for instance, will create a tripodal ligand where the three extended-arm binding-groups are nearly orthogonal to one another.

CTV can itself form coordination polymers with s-block metals through chelation to the metal cation through the dimethoxy groups.[28] This highlight article, however, will focus on coordination polymers employing tripodal and hexapodal CTV-type ligands combined with d- and f-block metals. CTV-ligands can be successfully embedded within coordination polymer materials, and a good proportion of such materials form with the desired hierarchical guest-binding spaces. However, this article will elucidate how the ability of CTV-type ligands to form host–guest interactions can, in fact, be counter-productive to forming materials with the hierarchical pores. Perspectives on successes will also be given – most particularly linked cage and capsule motifs, alongside tubular arrays, both of which are encouraged by the concave nature of the CTV-type ligands.

2. Crystalline host–guest behaviour of CTV-type ligands

Coordination polymers with CTV-type ligands have been formed from ligands with pyridyl, imidazole, allyl, pyridine-N-oxide, carboxylate, and catechol metal-binding functionality, shown in Chart 2. The types of coordination polymer formed by CTV-type ligands can be 1D chain, 2D or 3D, with 3D the least commonly observed. Some of the commonly occurring 2D network topologies for these networks are shown in Chart 3, classified by reticular chemistry structure resource nomenclature.[29] The host–guest associations formed by the CTV-type ligands in these materials are an important factor in determining the presence or otherwise of available guest-binding sites, so it is important to understand what types of host–guest or other associations these CTV-ligands may form.

The crystalline inclusion chemistry of the ligands in Chart 2 fall into three broad classifications: host–guest complexes with intra-cavity guest binding; and clathrate inclusion complexes where guests occupy lattice positions and there is either bowl-in-bowl stacking, or hand-shake motif self-inclusion of the CTV-ligands. It should be noted that a single ligand can form different types of inclusion complexes according to which guest is present.

Intra-cavity guest binding occurs where a molecular guest occupies the cavity of the host CTV-ligand, most commonly with a hydrophobic part of the guest molecule directed into the hydrophobic cavity of the host. Examples include (L2)·(MeNO$_2$),[21] (L9)·3.3(CH$_3$CN)·0.5(H$_2$O)[30] and (L19)·(DMF)[17] where DMF is dimethylformamide. Solvates of L10 have shown CHCl$_3$ (ref. 13) or Et$_2$O (ref. 16) (Fig. 1a) to be crystallographically characterised as intra-cavity guests, noting that in complex (L10)·(Et$_2$O)(NMP)$_2$ (ref. 16) additional N-methylpyrrolidone (NMP) occupies lattice sites. Interestingly, both (L2)·(MeNO$_2$) and (L10)·(Et$_2$O)(NMP)$_2$ form capsule-like head-to-head arrangements of host–guest complexes in the crystal lattice, shown for (L10)·(Et$_2$O)·1.5(NMP) in Fig. 1a. A similar capsule-like motif is seen for L1 crystallised from CH$_2$Cl$_2$/hexane however the presence of an intra-cavity guest could not be established crystallographically.[9]

Aligned bowl-in-bowl stacking occurs where columns of CTV-type ligands occur in the crystal lattice with ligands arranged on top of one another rather like a stack of soup bowls. Despite appearances, there are typically no π–π stacking interactions between the CTV-type molecules in such columns as separations between them are typically greater than 4.2 Å. The pyridyl-N-oxide ligands L17 and L19 each form clathrate materials with aligned bowl-in-bowl stacking in complexes (L17)·DMF (Fig. 1b) and (L19)·2(H$_2$O).[17] Each column is homochiral containing only one of the ligand enantiomers, however overall racemates are formed. Columnar stacking of ligands can also occur in an offset fashion where the orientation of the bowls are rotated and/or twisted with respect to one another, and often show inter-molecular interactions between the stacking ligands. This is nicely illustrated by the 4-pyridyl-appended L3 where different bowl-in-bowl stacks are formed from different crystallisation media. In one form, stacks of alternating enantiomers are formed with CH···π hydrogen bond formation (Fig. 1c), whereas a second form has significantly offset enantiomeric stacks.[29] Here one OMe group of each ligand is directed into the molecular cavity of another as the intracavity guest, and there are further face-to-face π–π stacking interactions, Fig. 1d. Ligands L5 (ref. 11) and L16 (ref. 31) also crystallise in offset bowl-in-bowl stacks.

The final category of host–guest motif is the hand-shake motif. This is a dimeric self-inclusion motif where the upper-rim extended arm of one host is directed into the molecular cavity of a second host and vice versa.[12] This usually occurs through an inversion centre to form a racemic hand-shake dimer, and π–π stacking interactions are often evident between the components. The clathrate complex (L8)·1.5(CHCl$_3$) is an

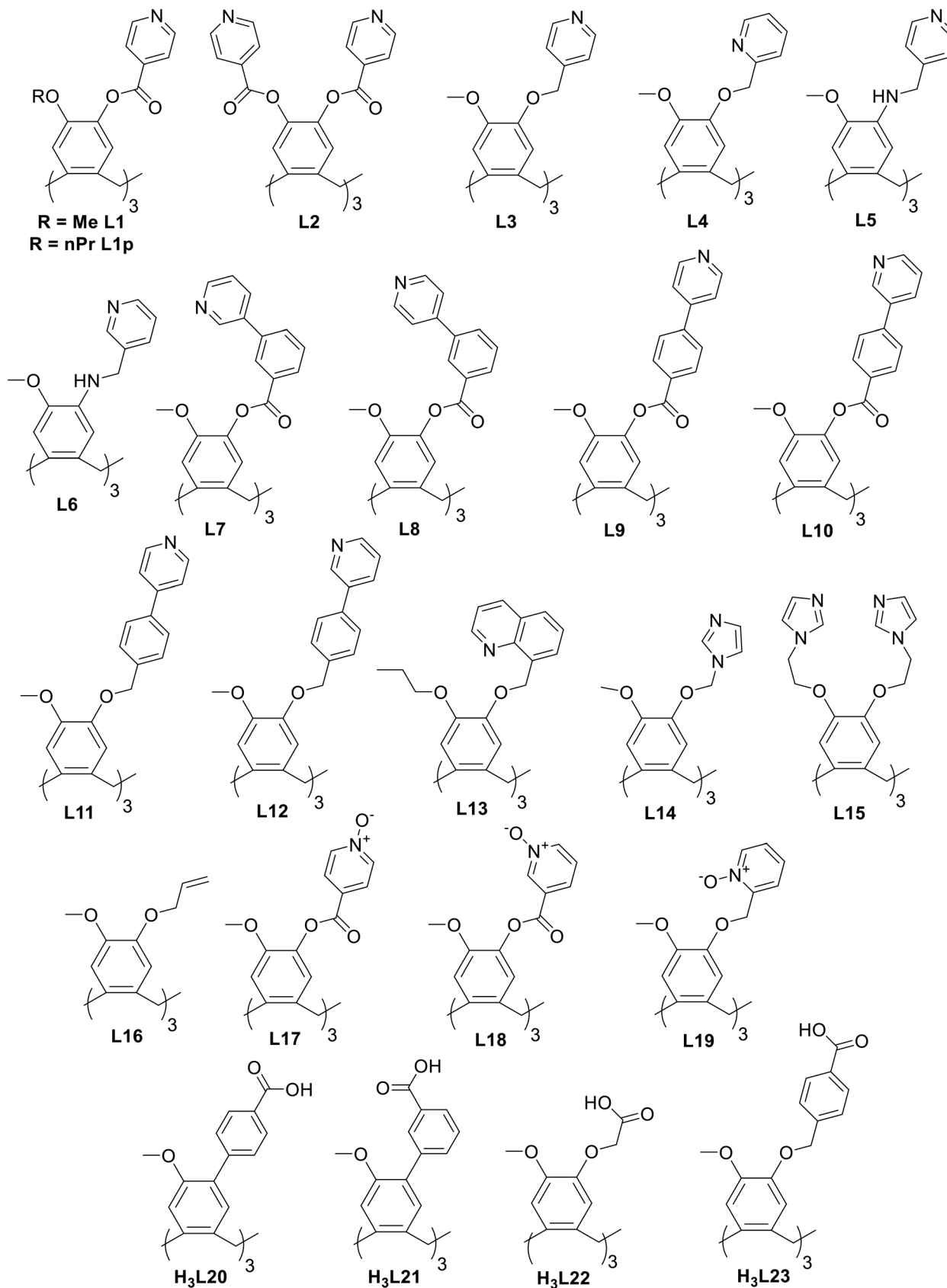**Chart 2** Functionalised CTV-type ligands known to form coordination polymers.

Chart 3 Most commonly occurring 2D topologies[29] for CTV-type coordination polymers.

Fig. 1 Crystal structures showing inclusion motifs of CTV-type ligands. (a) Intracavity host guest binding with capsule-like packing in (L10)·(Et$_2$O)·1.5(NMP) with guest Et$_2$O in space-filling mode;[29] (b) section of the lattice of (L17)·DMF showing aligned bowl-in-bowl stacking and clathrate inclusion of DMF (green).[17] Stacks are enantiomorphic but the crystal is a racemate with the orientation of the stacks (bowl-up, bowl-down) alternates in the lattice; (c) offset bowl-in-bowl stacking in one form of crystalline L3 with C–H···π hydrogen bond shown as red dashed line;[29] (d) offset bowl-in-bowl stacking in second form of L3 featuring host–guest associations with OMe group, additional π–π stacking shown as grey dashed line;[29] (e) the complementary self-inclusion hand-shake motif between two molecules of L8.[16]

illustrative example.[16] Here, one phenyl-pyridine group of the tris(3-(4-pyridyl)benzoyl)cyclotriguaiacylene (L8) host is directed into the cavity of another L8 host of opposite enantiomer, and *vice versa*, Fig. 1e. In another example, complex (L18)·2(NMP) features a hand-shake motif with face-to-face π–π stacking between pyridyl-*N*-oxide and bowl-aryl groups of the ligands.

3. Coordination polymers without post-construction guest-accessible host-sites

Known coordination polymers of CTV-type ligands with d- and f-block metals where the molecular cavity of the CTV-ligand is not accessible for any post-construction guest-binding are summarised in Table 1. The host–guest motifs observed for ligands and discussed in section 2 are also apparent within these coordination polymers, and are frequently the reason these materials do not exhibit hierarchical guest-binding space.

3.1 Bulky guests and host–guest directed assembly

As well as coordination polymers, the self-assembly of multi-topic bridging ligands with metal cations may result in the formation of discrete coordination capsule or cage structures.[32] There are a range of different coordination cages known with CTV-type ligands. Interestingly, the ability of the CTV-ligands to form host–guest interactions can direct whether a discrete species such as a cage, or a coordination polymer is the result of the self-assembly. For example, ligand L5 forms discrete species with Cd(OAc)$_2$ where OAc is acetate but addition of *ortho*-carborane results in formation of a [Cd(L5)(OAc)$_2$] 2D coordination polymer of 4·8^2 topology (**fes**) topology and with *ortho*-carborane guests, Fig. 2.[14] The ligand guest-binding sites cannot be considered guest-accessible for any post-construction manipulation as, by binding large guest molecules, they are effectively blocked. Likewise, ligand L5 forms a [Ag$_4$(L5)$_4$]$^{4+}$ tetrahedral coordination cage with

various Ag(I) salts, however addition of glutaronitrile to the reaction mixture results in the ultimate formation of a [Ag(L5)(NC(CH$_2$)$_3$CN)]$^+$ 2D coordination polymer again of **fes** topology.[11] Here, glutaronitrile molecules occupy the intra-cavity guest positions, Fig. S1.†

3.2 Intra- and inter-network host–guest associations with coordinated guest

If the metal coordination sphere is not saturated through coordination by the bridging CTV-type ligand then it may be coordinated by additional terminal ligands, such as anions or coordinated solvent. Coordinated solvent, in particular, has the potential to act as intra-cavity guest molecules for the CTV-type ligand as solvents which are frequently used for synthesis of these types of coordination polymers have the small hydrophobic groups that are typical guests for these ligands.

The presence of terminal ligands is most likely to occur with metals of high coordination number such as lanthanides. For example, the series of isostructural luminescent coordination polymers [M(L22)(DMF)$_2$], where M = Eu, Tb, Gd and L22 is a carboxylate-decorated CTV ligand, reported by Ma *et al.*, exhibit an intra-cavity host–guest association between a lanthanide-coordinated DMF and L22^{3-} ligand.[25] That lanthanide also binds to the carboxylate groups of the same L22^{3-} ligand.

CrystEngComm

Table 1 Coordination polymers with CTV-type ligands with inaccessible CTV host–guest site

Composition	Network	Inclusion motif	Ref.
$[Ag(L5)(NC(CH_2)_3CN)]\cdot n(NC(CH_2)_3CN)\cdot X$, X = $[Co(C_2B_9H_{11})_2]^-$, PF_6^-	2D, fes	Bulky guest	11
$[Cd(L5)(OAc)_2]\cdot(C_2B_{10}H_{12})\cdot(H_2O)$	2D, fes	Bulky guest	14
$[Ag_9(L16)_7(H_2O)_3]\cdot(L16)\cdot 9(SbF_6)$	3D	Bulky guest	15
$[Mn_6(OH)_3(ctc)_4]\cdot Cs_{10}Na_5(H_2O)_n$	3D, decorated pcu	Bulky guest	22
$[M(L22)(DMF)_2]$ M = Eu, Tb, Gd	1D, capsule-chain	Intra-chain coordinated guest	25
$[Eu(L23)(DMF)(H_2O)]\cdot 1.5(DMF)(H_2O)$	2D, decorated kgd	Intra-chain coordinated guest	18
$[Cu_2(L1)_2(OTf)_2(NMP)_2(H_2O)_2]\cdot 2(OTf)\cdot 2NMP$	2D, $(4\cdot 6^2\cdot 8)(6^2\cdot 8)(4\cdot 6^2\cdot 8^2)$	Inter-chain coordinated guest	20
$[Sm(L17)Cl(DMF)_3]\cdot[SmCl_5(DMF)]\cdot 1.5(DMF)$	1D ladder	Inter-chain coordinated guest	18
$[Cd_2(L9)(NO_3)_3(H_2O)_2(DMA)_2]\cdot(NO_3)\cdot(DMA)$	1D chain	Inter-chain coordinated guest	16
$[Ag_2(L16)_2]\cdot 2(SbF_6)$	3D	Aligned bowl-in-bowl (intra)	15
$[Yb(L22)(H_2O)(DMF)]$	3D, rtl	Rotated bowl-in-bowl (intra)	25
$[Ag_2(L16)(H_2O)_2]\cdot 2(BF_4/ClO_4)\cdot 2(MeNO_2)$	1D	Bowl-in-bowl (intra, rotated)	15
$[Ag_2(L16)(CF_3SO_3)_2]$	3D	Offset bowl-in-bowl (intra, OMe guest)	15
$[Ag(L16)(CF_3SO_3)]$	2D	Offset bowl-in-bowl (intra, OMe guest)	15
$[Cu(L1)(NCMe)]\cdot BF_4\cdot 1.5(CH_3CN)\cdot 2(H_2O)$	2D, hcb	Aligned bowl-in-bowl (inter)	20
$[M_2(OAc)(L20)(DMF)]$ M = Zn, Co	2D decorated hcb	Aligned bowl-in-bowl (inter)	24
$[M(L19)(NO_3)_2]\cdot 2(DMF)$ M = Zn, Cd	2D, hcb	Isolated CTV sites	17
$[Ag_2(L13)_2]\cdot[Co(C_2B_9H_{11})]_2\cdot 1.5(NO_2Me)$	1D chain	Infinite hand-shake	19
$[Ag(L14)]\cdot ReO_4\cdot CH_3CN$	1D chain	Linked hand-shake	12
$[Ag(L12)]\cdot SbF_6\cdot 3(DMF)\cdot H_2O$	1D chain	Linked hand-shake	12
$[Ag(L6)(H_2O)]\cdot SbF_6$	1D chain	Linked hand-shake	11
$[M(L7)(NO_3)_2]\cdot 4(NMP)$ M = Co, Zn	1D ladder	Intra-chain hand-shake	16
$[M(L18)_2(DMF)_2]\cdot 2ClO_4\cdot 8(DMF)$ M = Cu, Cd	2D, sql	Intra-network hand-shake	17
$[Gd(L19)(NO_3)_3]\cdot DMF$	1D ladder	Inter-chain hand-shake	18
$[Co(L18)_2(DMF)_2]\cdot 2NO_3\cdot 4(DMF)\cdot H_2O$	1D chain	Inter-chain hand-shake	17
$[Co_2(L8)_2(NO_3)_2(H_2O)_5]\cdot 2(NO_3)\cdot n(DMF)$	2D, bex	Inter-network hand-shake	16

See Chart 2 for ligand numbering; ctc = catecholate of CTC (Chart 1); NMP = N-methylpyrrolidone; DMF = N,N-dimethylformamide; DMA = N,N-dimethylacetamide; intra = intra-network association; inter = inter-network association.
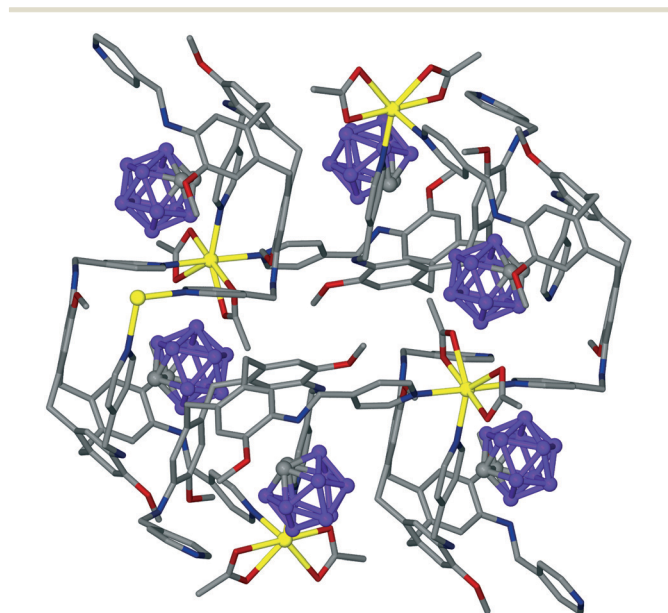
$[M(L22)(DMF)_2]$ form 1D chain structures with dimeric clusters of lanthanide cations held together by four $L22^{3-}$ ligands. The ligands are orientated such that a chain of dimeric capsules are formed, Fig. 3a. Overall packing of the chains leaves only small

Fig. 2 Section of the crystal structure of $[Cd(L5)(OAc)_2]$ showing formation of 2D network and host–guest binding of $C_2B_{10}H_{12}$ o-carborane guests (purple). Hydrogen atoms excluded.[14]

cavities in the lattice, Fig. S2.† Nevertheless, an aqueous suspension of the Eu and Tb materials show selective luminescence quenching in the presence of Fe^{3+} or MnO_4^- which occurs without structural changes.[25] A further example of a material with an intra-chain coordinated host–guest motif is found in $\{[Eu(L23)(DMF)(H_2O)]\cdot 1.5(DMF)(H_2O)\}$[18] which utilises a distinct carboxylate-decorated CTV ligand. The structure features a carboxylate-bridged Eu-dimer with terminal DMF and aquo ligands. Each Eu-dimer is coordinated by six $L23^{3-}$ ligands to form a 2D decorated kagome dual (**kgd**) network. Coordinated DMF ligands occupy every CTV guest-site, Fig. 3b.

Coordinated N-methyl pyrrolidone (=NMP) ligands act as guest molecules in an inter-network host–guest motif in complex $[Cu_2(L1)_2(OTf)_2(NMP)_2(H_2O)_2]\cdot 2(OTf)\cdot 2(NMP)$.[20] The 2D network is two-tiered with 3,4-connectivity and a network that resembles linked open tubes forms when viewed down the a axis, Fig. 4a. There are two crystallographically independent L1 ligands, one of which does bind an uncoordinated NMP and is shown in pink in Fig. 4a. the other, however forms host–guest interactions with coordinated NMP of interpenetrating networks leading to a material without substantial pores, Fig. 4b.
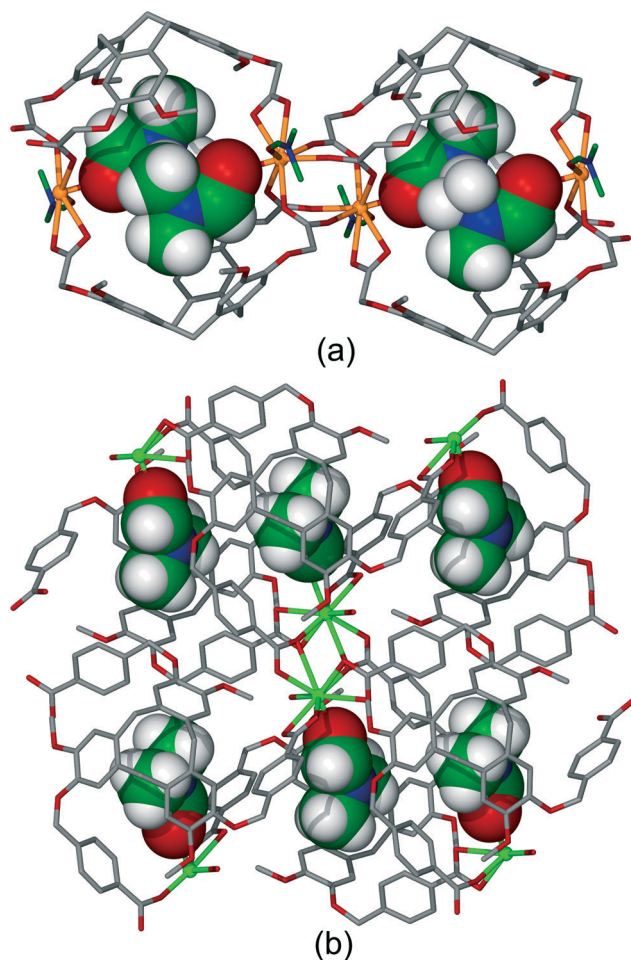
3.3 Self-inclusion motifs

Bowl-in-bowl self-inclusion motifs can occur between 2D coordination networks or within a 3D network. For example, aligned bowl-in-bowl stacking within a single 3D network is
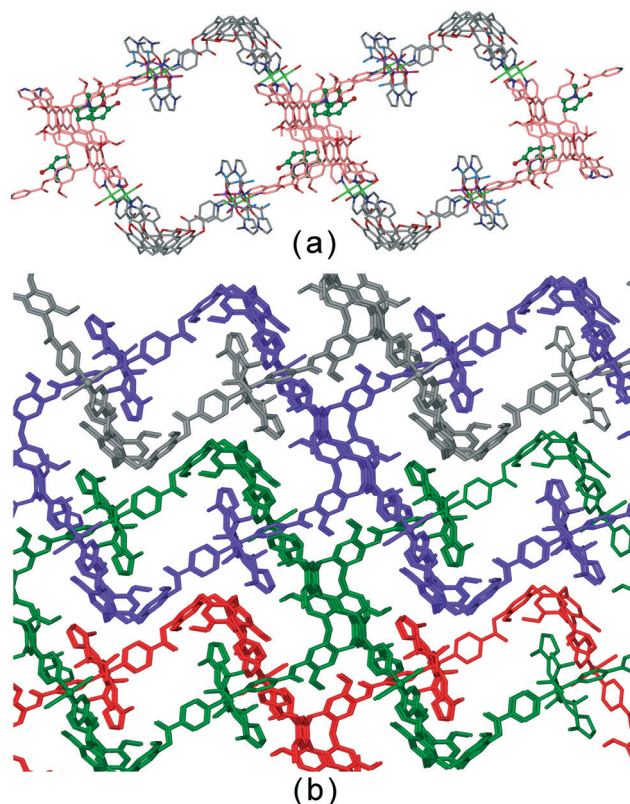
Fig. 3 Intra-cavity host–guest associations between a coordinated DMF guest and carboxylate-decorated CTV ligand within a single network or chain in (a) [Eu(L22)(DMF)$_2$] chain structure;[25] (b) section of the 2D network of {[Eu(L23)(DMF)(H$_2$O)]·1.5(DMF)(H$_2$O)}.[18] DMF are shown in space-filling.

Fig. 4 Crystal structure of [Cu$_2$(L1)$_2$(OTf)$_2$(NMP)$_2$(H$_2$O)$_2$]·2(OTf)·2(NMP).[20] (a) Highlight of a single [Cu$_2$(L1)$_2$(OTf)$_2$(NMP)$_2$(H$_2$O)$_2$]$^{2+}$ network with L1 ligands that bind uncoordinated NMP in pink with NMP guests in ball-and-stick; (b) packing diagram with solvent guest and anions excluded showing interpenetrating networks in different colours, and inter-network host–guest associations.

observed in complex [Ag(L16)]·(SbF$_6$).[15] The [Ag(L16)]$^+$ network is a 3-connected network which shows large hexagonal channels that contain disordered SbF$_6^-$ anions. The walls of the channels are helical, and have aligned enantiomeric bowl-in-bowl stacks of L15 ligands, Fig. 5a. As for examples of such stacking with ligands alone, there is no indication of π–π stacking between the CTV-type bowls. Bowl-in-bowl stacking motifs are also seen for other Ag(I) organometallic polymers with L16 (Table 1). The luminescent [Yb(L22)(H$_2$O)(DMF)] reported by Ma et al.,[25] also has a 3D coordination polymer structure with bowl-in-bowl stacking, in this case offset and with alternating ligand enantiomer, Fig. 5b. The material does not contain significant pores or channels. The complexes [M$_2$(OAc)(L20)(DMF)$_2$] where M = Zn or Co reported by Easun and Schröder et al.,[24] feature 2D coordination polymers with carboxylate-bridged metal-dimers linked by the carboxylate-decorated CTV-type ligand L20^{3-} into a hexagonal network of decorated 6^3 topology (**hcb**). Each network contains both ligand enantiomers and the orientation of the ligand bowl (up or down) alternates. These
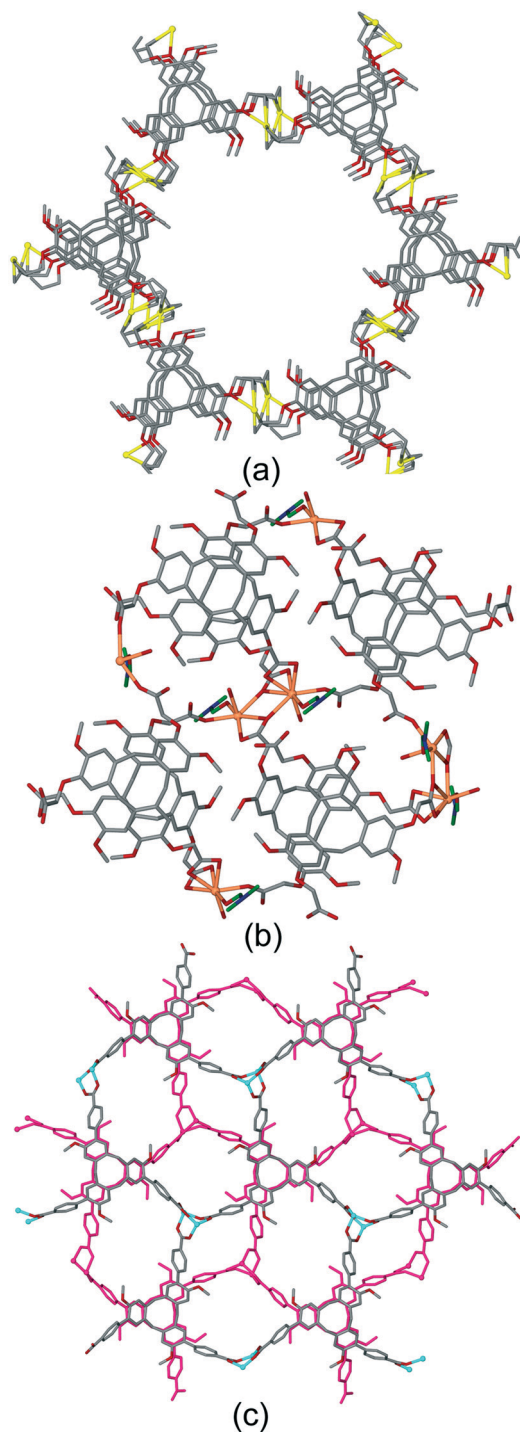
2D networks stack through bowl-in-bowl stacking of racemic ligands of adjacent networks with an AB stacking pattern. This stacking pattern significantly reduces the channel size inherent in the networks, Fig. 5c. Aligned bowl-in-bowl stacking between **hcb** networks is also found for [Cu(L1)(NCMe)]·BF$_4$·1.5(CH$_3$CN)·2(H$_2$O)[20] which is similar to [M$_2$(OAc)(L20)(DMF)$_2$] in terms of network achirality, orientation of the ligand bowls and network stacking. Network stacking also effectively blocks any potential porosity for {[M(L19)(NO$_3$)$_2$]·2(DMF)} where M = Zn, Cd.[17] This material also forms a 2D network of **hcb** topology, and the material is a conglomerate with each single crystal containing only one enantiomer. The conformation of one pyridine-N-oxide side arm prevents direct bowl-on-bowl stacking of networks and the [M(L19)(NO$_3$)$_2$] networks are stacked such that a small cavity of approximately 44 Å^3 volume is created at the CTV bowl, however these cavities are isolated within the lattice, Fig. S3.†
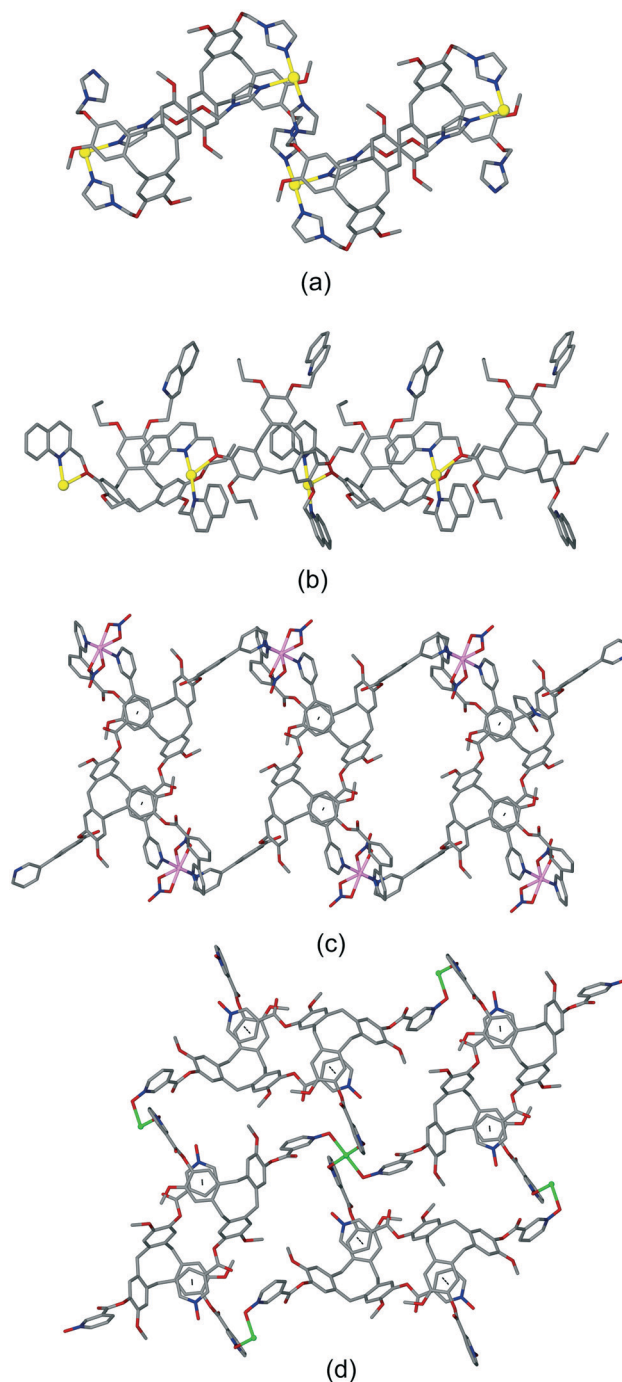
The hand-shake self-inclusion is also a recurrent motif in coordination polymers involving CTV-type ligands. In chain-like 1D coordination polymers it is observed as either linked pairs of hand-shake dimers, or as an infinite chain of non-dimeric associations. An example of the former is seen in

(a)

(b)

(c)

Fig. 5 Examples of crystal structures showing bowl-in-bowl stacking in coordination polymers. (a) Section of 3D network showing one hexagonal channel in $[Ag(L16)]·(SbF_6)$ with intra-network bowl-in-bowl stacking;[15] (b) the 2D network of $[Yb(L22)(H_2O)(DMF)]$ with intra-network bowl-in-bowl stacking;[25] (c) stacking of 2D hexagonal networks in $[Zn_2(OAc)(L20)(DMF)_2]$ with terminal ligands excluded and one network shown in pink for clarity.[24]

(a)

(b)

(c)

(d)

Fig. 6 Intra-chain or intra-network hand-shake host–guest motifs (a) linked pair-wise hand-shake of $[Ag(L14)]^+$;[12] (b) infinite non-pairwise hand-shake of $[Ag_2(L13)_2]^{2+}$;[19] (c) ladder structure of $[Co(L7)(NO_3)_2]$ with π-stacking interactions at 3.80 Å within each hand-shake pair indicated as dashed lines;[16] (d) section of the 2D $\{[Cu(L18)_2(DMF)_2]^{2+}$ network with π-stacking interactions at 3.55 Å within each hand-shake pair indicated as dashed lines, and coordinated DMF excluded for clarity.[17]

$[Ag(L14)]·ReO_4·CH_3CN$ (ref. 12) and illustrated in Fig. 6a. The 1D chain within complex $[Ag_2(L13)_2]·[Co(C_2B_9H_{11})]_2·1.5(NO_2Me)$ (Fig. 6b)[19] illustrates the other infinite hand-shake motif where

each L13 ligand acts as a host for one other L13 within the chain and as a guest for a different L13 molecules within the chain. The 1D ladder structures of $[M(L7)(NO_3)_2]·4(NMP)$ where M = Co, Zn (ref. 16) also form pair-wise hand-shake motifs with

face-to-face π-stacking interactions, Fig. 6c. An intra-network hand-shake association is also observed for the 2D coordination polymer of [M(L18)$_2$(DMF)$_2$]·2ClO$_4$·8(DMF) where M = Cu, Cd.[17] Here, an uncomplexed pyridine-N-oxide side-arm of each L18 ligand acts as the guest component and forms face-to-face π-stacking interactions with an arene group of its partner host CTV-core, Fig. 6d. Each association is dimeric with pairwise host–guest associations. Hand-shake motifs also occur between chain coordination polymers (Table 1) and between the 2D coordination networks of [Co$_2$(L8)$_2$(NO$_3$)$_2$(H$_2$O)$_5$]·2(NO$_3$)·n(DMF). The latter has a 3,4-connected network of $(4^2 \cdot 6^2)(4 \cdot 6^2)_2$ (**bex**) topology and pair-wise hand-shake associations occur between L8 ligands of different networks leading to 2D-to-3D polycatenation, Fig. S4.†[16]

4. Coordination polymers with differential guest–accessible sites

While host–guest interactions or self-association motifs lead to the effective blockage of the molecular recognition site in a number of coordination polymers with CTV-type ligands, there are a sufficient number of materials where both guest-binding modes are available to begin to establish trends. Known examples are summarised in Table 2. The formation of coordination capsules or cage-like entities within the coordination polymer is one such trend, as is the formation of tubular-like structures either by 1D chain or 2D networks.

4.1 Linked capsules and cages

The bowl-like nature of CTV and its analogues makes it an excellent building-block for discrete cage-like assemblies. Examples include metal–organic or coordination cages,[32] alongside covalently linked capsules such as cryptophanes[27,33] and larger cages,[34] and hydrogen-bonded capsules.[35] Networked coordination cages – where coordination polymers are composed of linked cage motifs – are one of the principal classifications of coordination polymers of CTV-analogue ligands with guest-accessible molecular recognition sites and lattice-type guest sites. Other bowl-shaped host molecules of the calixarene-family have also been shown to form MOFs/coordination polymers with embedded metallo-capsules,[6] and Atwood and co-workers have also reported much larger network nano-cages with pyrogallol[4]arene hosts.[7] Holman et al. have also reported a coordination chain material with embedded cryptophanes which are organic CTV-based capsules.[36] The earliest examples with CTV-ligands were the series [Ag$_3$(L10)$_2$(CH$_3$CN)$_3$Cl]·2X·n(CH$_3$CN) where X = BF$_4$, AsF$_6$ or ClO$_4$.[13] The 2D [Ag$_3$(L10)$_2$(CH$_3$CN)$_3$Cl]$^{2+}$ network features {Ag$_3$(L10)$_2$} trigonal bipyramidal coordination capsules, also known as metallo-cryptophanes, linked into a hexagonal network through a bridging μ$_3$-Cl$^-$ with trigonal planar geometry, shown in Fig. 7. Formation of this network was serendipitous as the Cl$^-$ anion was sourced from a small amount of the

Table 2 Coordination polymers with CTV-type ligands with accessible CTV host–guest and lattice guest sites

Compound	Network	Descriptor	Ref.
[Ag$_3$(L10)$_2$(CH$_3$CN)$_3$Cl]·2X·n(CH$_3$CN), X = BF$_4$, AsF$_6$, ClO$_4$	2D, decorated hcb	Network of capsules	13
[Cu$_3$(L3)$_4$(H$_2$O)$_3$]·6(OTf)·n(DMSO)	2D, decorated hcb	Network of capsules	20
[Zn$_6$(L21)$_4$(DMA)$_6$(H$_2$O)$_5$]	2D, decorated hcb	Network of capsules	24
[{Re(CO)Br}$_3$(L2)$_2$]	2D, decorated hxl	Network of capsules	21
[{M(H$_2$O)$_2$}$_3$(L2)$_2$]·6(NO$_3$) M = Co, Cu, Ni	2D, decorated hxl	Network of capsules	21
[{Co(X)$_2$}$_3$(L2)$_2$], X = Cl, Br, I	2D, decorated hxl	Network of capsules	21
[Cu$_2$(L11)$_2$Br$_2$(H$_2$O)(DMSO)]·2Br·n(DMSO)	1D chain	Linked capsules	20
[Ag$_3$(NMP)$_6$(L17)$_2$]·3(ClO$_4$)·n(NMP)	3D, pyr	Cage-like assembly	17
[Cu$^I_4$Cu$^{II}_{1.5}$(L1)$_3$(CN)$_6$]·CN·n(DMF)	3D	Cage-like assembly	20
[M$_3$(L15)(BDC)$_3$]·DMF·6(H$_2$O), M = Zn, Cd	3D, decorated acs	Cage-like assembly, interpenetrating	26
[Cu$_3$(L20)$_2$(EtOH)(PY)$_2$(H$_2$O)$_2$]·9(DEF)·8(H$_2$O)	1D, bex	Tubular, interpenetrating	23
[Ag(L1p)[Co(C$_2$B$_9$H$_{11}$)$_2$]]·2(DMF)·(H$_2$O)	1D ladder	Tubular	19
[Cd(L1p)(NO$_3$)$_2$(H$_2$O)]·DMF·2(Et$_2$O)	2D, fes	Two-tiered	19
[Cu$_2$(L3)$_2$Br$_3$(DMSO)]·Br·n(DMSO)	2D, fes	Two-tiered	20
{[M(L17)$_2$]·2(BF$_4$)·n(NMP)} M = Zn, Co	2D, kgd	Two-tiered	17
[Cu(L17)$_2$]·[Cu(H$_2$O)(NMP)$_4$]·4(BF$_4$)·8(NMP)·2(H$_2$O)	2D, kgd	Two-tiered	17
[Cu$_2$(L2)(TFA)$_3$(INIC)]	2D	Two-tiered	21
[Ag(L1)$_2$]·[Co(C$_2$B$_9$H$_{11}$)$_2$·9(CH$_3$CN)	1D double-bridged chain	CH$_3$CN intracavity and lattice guests	9
[Zn(L9)$_2$(CF$_3$COO)(H$_2$O)]·(CF$_3$COO)·7(NMP)	1D double-bridged chain	NMP intracavity guests, lattice channels	16
[Ag$_2$(L2)(DMF)$_2$]·2(BF$_4$)·2(H$_2$O)	2D, kgd	DMF intracavity and lattice guest	21
[Cu$_5$(L19)$_2$Cl$_{10}$(NMP)$_4$]·n(NMP)	2D decorated hcb	NMP intracavity guest, large channels	17
[Cd$_2$(L9)$_2$(NO$_3$)$_4$(NMP)]·9(NMP)·4(H$_2$O)	2D, bex	NMP guests, 4-fold interpenetrating	16
[Co(L9)(H$_2$O)$_2$]·2(NO$_3$)·2(DMF)	2D, bex	DMF guests, 4-fold interpenetrating	16
[Ag$_3$(L4)$_2$]·3(PF$_6$)	3D, srs	PF$_6$$^-$ intracavity and lattice guests	10
[Cu$_2$(L1)$_2$(NMP)(H$_2$O)]·4(BF$_4$)·12(NMP)·1.5(H$_2$O)	3D, ths	NMP intracavity and lattice guests, 2-fold interpenetrating	20

See Chart 2 for ligand numbering; NMP = N-methylpyrrolidone; DMF = N,N-dimethylformamide; DEF = N,N-diethylformamide; DMA = N,N-dimethylacetamide; BDC = benzene-1,3-dicarboxylate; PY = pyridine; TFA = trifluoroacetate; INIC = isonicotinate.

Fig. 7 From the structure of $[Ag_3(L10)_2(CH_3CN)_3Cl]\cdot 2AsF_6\cdot n(CH_3CN)$ showing the 2D network of Ag_3L_2 capsules linked by μ_3-Cl^- (larger olive spheres) and inset is side-view of one capsule highlighting that the μ_3-Cl^- are *endo* to the cage.[13]

hydrochloride salt of the L10 ligand that was present in the bulk L10 sample used. Simple addition of a Cl^- salt would lead to AgCl formation. The extended phenyl-pyridyl arms of L10 mean that the capsules are inherently large (*ca.* 18 Å in length axially and 11 Å from equatorial Ag to capsule centre), while disordered anions (only located for the AsF_6^- example) occupy the equatorial central space of the capsule. The overall crystal lattice does exhibit connected channels but these are relatively small, Fig. S5.†

The complex $[Cu_3(L3)_4(H_2O)_3]\cdot 6(OTf)\cdot n(DMSO)$ also features a network of linked trigonal bipyramidal M_3L_2 capsules.[20] Here the capsules are directly linked together through shared Cu(II) apices (Fig. 8a), to form a 3,4-connected 2D network of a hexagonal array of capsules with very large cavities, Fig. 8b. A structurally very similar 2D network of M_3L_2 cages has also been reported by Tian and co-workers.[37] In that material, the ligand is 1,1′,1″-((2,4,6-trimethylbenzene-1,3,5-triyl)tris(methylene))tris (pyridine-1-ium-4-carboxylate) which adopts a bowl-conformation not dissimilar to that of CTV. For $[Cu_3(L3)_4(H_2O)_3]^{6+}$ the longest Cu···Cu distance across this cavity is 34.1 Å, and the cavity is lined with terminal aquo ligands bound to apical positions of the square pyramidal Cu(II) centres. The $[Cu_3(L3)_4(H_2O)_3]^{6+}$ layers pack in an AB manner and there are large channels running through the lattice, Fig. 8c, with the ordered $[Cu_3(L3)_4(H_2O)_3]^{6+}$ layers only occupying around 20% of the unit cell volume. The crystals were not robust and the network collapses on solvent loss. Despite this, the material is stable

if kept under solvent and can be used as a crystalline sponge, and uptake of fullerene C_{60} from toluene solution has been demonstrated.

The complex of the carboxylate-decorated CTV ligand, $L21^{3-}$, $[Zn_6(L21)_4(DMA)_6(H_2O)_5]$, where DMA = *N,N*-dimethylacetamide, reported by Easun and Schröder also features capsule motifs linked into a hexagonal 2D array, Fig. 9a and b.[24] In this case the capsules are linked through a $Zn_2(carboxylate)_4$ dimer with the well-known paddle-wheel structural motif. The capsules of the as-synthesised material contain free and coordinated DMA molecules and there are linked pores throughout the lattice, Fig. S6.† All three of these 2D networks of capsules have the same, common 6^3 (**hcb**) topology if the capsule is regarded as a decorated connecting node. The hexapodal ligand L2 featuring six isonicotinoyl ligand groups also forms 2D networks of linked cryptophane-like capsules, however with quite different topology to the hexagonal **hcb** network. For example [{Re(CO)Br}$_3$(L2)$_2$] forms linked M_6L_2 capsules with each capsule linked to six others through vertex-sharing at the Re(I) centres. The network thus formed has decorated 3^6 (**hxl**) hexagonal topology if each capsule is considered a connecting centre, Fig. 9c.[21] As for $[Zn_6(L21)_4(DMA)_6(H_2O)_5]$, the framework is neutrally charged and packing occurs in a manner to create linked channels through the lattice, Fig. S7.† Uncomplexed nitromethane can be resolved within the capsule of the as-synthesised material and [{Re(CO)Br}$_3$(L2)$_2$]$\cdot n(CH_3NO_2)$ is robust to solvent evacuation. It can uptake I_2 from solution with approximately 1.5 molecules of I_2 absorbed per capsule. A series of isostructural complexes [{M(H$_2$O)$_2$}$_3$(L2)$_2$]·6(NO$_3$) (M = Co, Cu, Ni) and [{Co(X)$_2$}$_3$(L2)$_2$] (X = Cl, Br, I) feature the same **hxl** 2D network as [{Re(CO)Br}$_3$(L2)$_2$] although have distinct lattice packing, Fig. S8.†[21] Tripodal CTV-type ligands can also form chains of linked M_3L_2 capsules.[20]

Robson and co-workers have reported a CTC-based coordination polymer, $[Mn_6(OH)_3(ctc)_4]\cdot Cs_{10}Na_5(H_2O)_n$ where ctc is deprotonated cyclotricatechylene. This features tetrahedral cages linked together into a network through Mn–OH–Mn hydroxide bridges and $Cs^+\cdots\pi$ interactions, Fig. 10.[22] The space within the tetrahedron is occupied by a $\{Cs_4(Na(H_2O)_6)\}$ cluster which also forms π-interactions to the ctc, thus this material is best regarded as an example of a bulky guest blocking CTV-type sites (Table 1). Nevertheless, it points to interesting linked-cage topologies that can be accessed using CTV-type ligands.

It should be noted that in all of these examples, cage-assemblies within these coordination polymers are formed concomitantly with formation of the network itself. There are no examples of pre-formed discrete metal–organic cages which features CTV-type ligands being subsequently linked into network structures. This is also the case for networked coordination capsules and coordination cages with other host molecules.[6,7] As for the CTV examples, these included networks of vertex-linked capsules as well as those linked by an additional ligand. Examples of post-synthetic assembly of
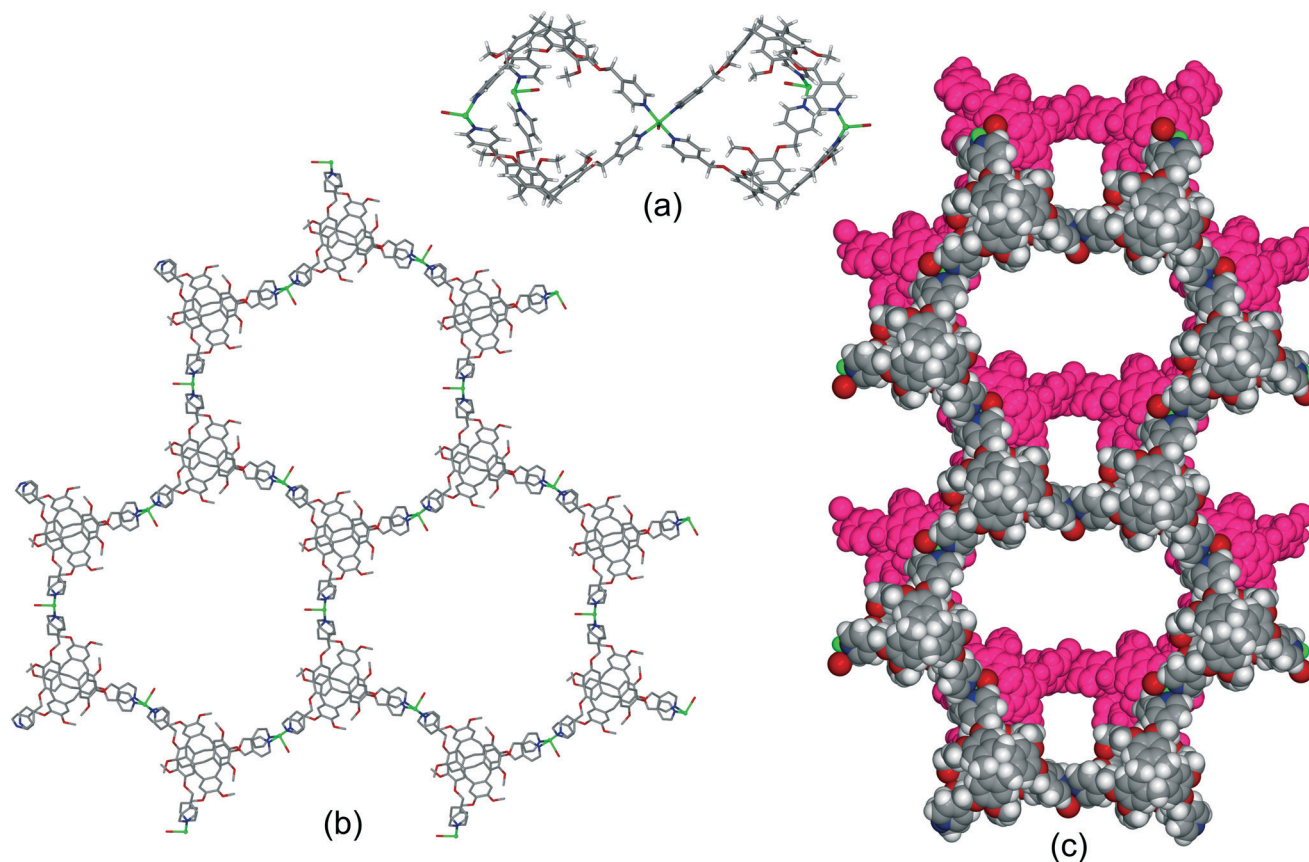
Fig. 8 Crystal structure of $[Cu_3(L3)_4(H_2O)_3]\cdot6(OTf)\cdot n(DMSO)$. (a) Two Cu_3L_2 capsules linked through a shared Cu(II)–vertex; (b) 2D network of linked capsules; (c) packing of two network layers (one in pink) showing substantial channels with largest ca. 1.5 × 3 nm cross-section.[20]

pre-formed coordination cages of any type into crystalline MOF or coordination polymer materials are rare.[38] Post-synthetic organisation of coordination cages can also target soft materials.[39]

Coordination polymer networks with available CTV-ligand binding sites also occur where more complicated cage-like assemblies are formed within the network. Complex $[Ag_3(NMP)_6(L17)_2]\cdot3(ClO_4)\cdot n(NMP)$ utilises a tripodal CTV ligand with pyridine-*N*-oxide metal-binding groups.[17] The basic framework is a 3D $[Ag(L17)_2]^+$ coordination polymer of 3,6-connectivity and pyrite (**pyr**) topology with the Ag(I) octahedrally coordinated by L17 ligands. Cage-like pores form with two L17 ligands in a head-to-head arrangement bridged by six Ag–L17–Ag connections, Fig. 11a. All L17-ligands within the network are crystallographically identical so a network of linked pores is created. An extraordinary aspect of this material is that each Ag(I) connecting centre also forms argentophilic interactions to two $[Ag(NMP)_3]$ fragments at Ag···Ag separation 3.275 Å. The complex $[Cu^I_4\text{-}Cu^{II}_{1.5}(L1)_3(CN)_6]\cdot CN\cdot n(DMF)$ has a heteroleptic coordination polymer structure with bridging L1 and cyanide ligands and a complicated 3,4-connected 3D topology which features linked hexagonal prismatic cages, Fig. 11b.[20] A further heteroleptic coordination polymer has been reported by Ma *et al.* using the hexapodal imidazole-decorated ligand L15 in

$[Cd_3(L15)(BDC)_3]\cdot DMF\cdot6H_2O$ where BDC is benzene-1,3-dicarboxylate.[26] $[Cd_3(L15)(BDC)_3]$ forms an intricate 3D coordination polymer that contains the BDC-expanded capsule-motifs shown in Fig. 11c. Each of these capsules is linked to six others in a trigonal prismatic fashion through the BDC ligands shown *exo* to the expanded cages in Fig. 11c, to form a cage-decorated **acs** network, Fig. S9.† The network can also be reduced to a $(6\cdot10^2)_3(6^3)$ net if L15 and metal positions are considered as 3-connectors, Fig. S9.† The material shows four-fold interpenetration but has substantial channels nevertheless, Fig. S10.† It shows both single-crystal-to-single-crystal guest exchange properties, and catalyses Knoevenagel condensation and CO_2 cycloaddition reactions.

4.2 Two-tiered and tubular arrangements

A further notable category of structure where there are pathways through the lattice and the host molecular recognition sites are guest-accessible, are those where tubular CTV-ligand-lined channels are formed. These occur because the bowl-like CTV ligands do not form flat networks, and there is often a concave–convex aspect to the net with bowls inverted with respect to one another. This can create two-tier chains and networks with the CTV-bowls oriented inwards when viewed down the channel axis.
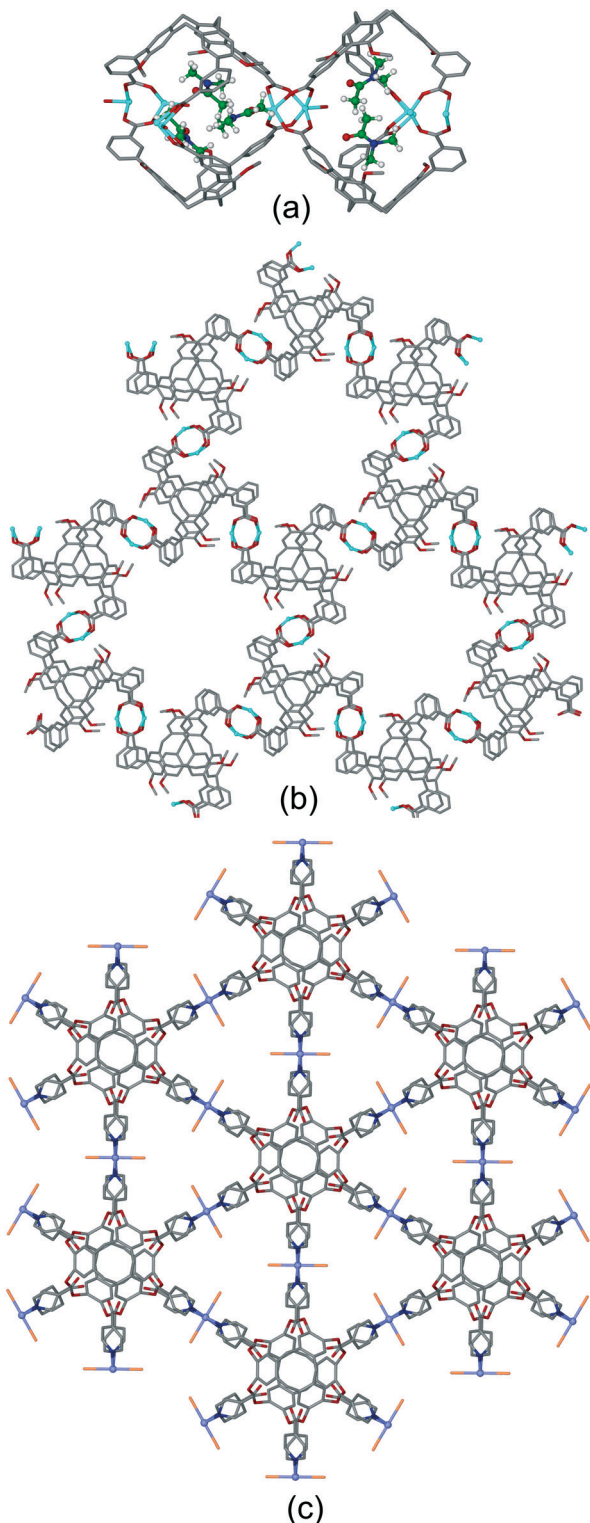
(a)

(b)

(c)

Fig. 9 Other examples of hexagonal networks of capsules. (a) Two paddle-wheel linked capsules of $[Zn_6(L21)_4(DMA)_6(H_2O)_5]$ showing included DMA as ball-and-stick, (b) network of $[Zn_6(L21)_4(DMA)_6(H_2O)_5]$ with terminal ligands excluded;[24] (c) decorated hxl-network of $[\{Re(CO)Br\}_3(L2)_2]$, terminal ligands are disordered Br/CO.[21]

Zheng and co-workers have reported $[Cu_3(L20)_2(EtOH)(PY)_2(H_2O)_2] \cdot 9DEF \cdot 8H_2O$ where PY is pyridine which has a
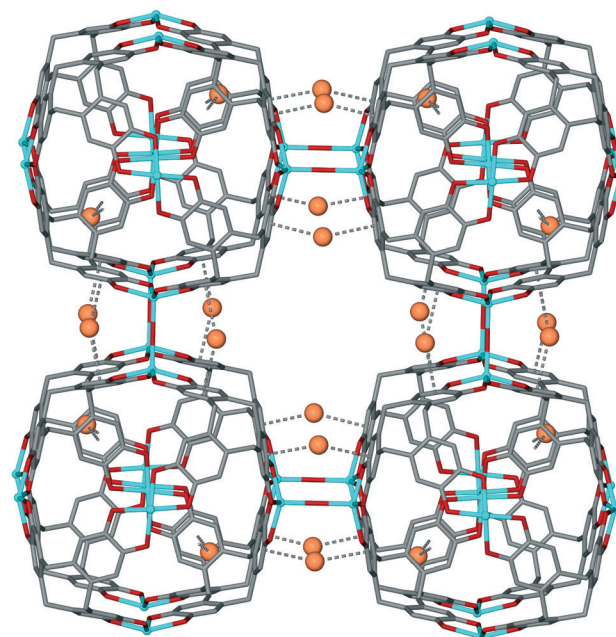

Fig. 10 3D coordination polymer of $[Mn_6(OH)_3(ctc)_4] \cdot Cs_{10}Na_5(H_2O)_n$ with water and Cs/Na positions inside the $[Mn_6(ctc)_4]$ cage excluded. Disordered bridging OH is shown in averaged position, and $Cs^+ \cdots \pi$ interactions as dashed lines.[22]

tubular coordination chain structure, shown in Fig. 12.[23] The structure is interpenetrating and two entangled chains are orthogonal to one another such that Cu-pyridyl lined channels occur. Robust porosity of the material was demonstrated by N_2 sorption which indicated a pore diameter of 6.04 Å, consistent with the crystal structure. $[Ag(L1p)[Co(C_2B_9H_{11})_2]] \cdot 2(DMF) \cdot (H_2O)$ is an example of a tubular 1D coordination polymer where there is no interpenetration and DMF guests molecules occupy both CTV-intracavity sites and lattice positions, Fig. S11.†[19]

Most other examples are 2D coordination polymers, and occur with the formation of distinctly two-tiered coordination polymers. One such example is $[Cd(L1p)(NO_3)_2(H_2O)] \cdot DMF \cdot 2Et_2$-O where a 3-connected 2D coordination polymer of **fes** topology is formed, with uni-directional CTV-lined channels.[19] Distinct guest-binding could be elucidated with DMF occupying the CTV-ligand molecular bowl and diethylether in lattice-guest sites, Fig. 13a. Complex $[Cu_2(L3)_2Br_3(DMSO)] \cdot Br \cdot n(DMSO)$ also has a 2D network of **fes** topology which is highly kinked to give a two-tiered structure, Fig. S12.† Complexes $[M(L17)_2] \cdot 2BF_4 \cdot n(NMP)$ where M = Zn or Co are isostructural, and there is also a Cu(II)-variant.[17] They feature 2D coordination polymers of 3,6-connected **kgd** topology. The network is two-tiered and forms tubular CTV-lined channels that run in two orthogonal directions, Fig. 13b. The **kgd** topology is relatively rare. A pyridyl-appended CTV-ligand such as L1 would not form such a network with an octahedral metal due to steric clash of pyridyl groups. The N-oxide derivative L17, on the other hand, can do so due to the near 90° N–O–M coordination angle, with L17 acting as the 3-connecting centre. The hexapodal ligand L2 forms a different type of 2D coordination polymer with the two-

Fig. 11 Examples of cage-like assemblies. (a) [Ag$_3$(NMP)$_6$(L17)$_2$]·3(ClO$_4$)·n(NMP): [Ag(L17)$_2$]$^+$ framework showing cage-like pore bounded by two head-to-head L16-ligands (in green); inset shows full coordination sphere of connecting Ag(I) showing decoration by two [Ag(NMP)] moieties. NMP shown in green, only one L17 shown in full for clarity;[17] (b) linked hexagonal prisms within the [Cu$^I_4$Cu$^{II}_{1.5}$(L1)$_3$(CN)$_6$]$^+$ 3D network structure, all Cu centres (green spheres) are either 3 or 4-coordinate with edge-shared along the Cu–CN–Cu chains occurring between prisms above and below those shown, carbon atoms of cyanide ligands shown in purple;[20] (c) expanded capsule-like motif within the 3D coordination network of [Cd$_3$(L15)(BDC)$_3$], structure is 4-fold interpenetrating.[26]

tiered aspect required for tubular channels in the heteroleptic complex [Cu$_2$(L2)(TFA)$_3$(INIC)] (where TFA = trifluoroacetate, INIC = isonicotinate).[21] Each L2 ligand in [Cu$_2$(L2)(TFA)$_3$(INIC)] coordinates through five of its six pyridyl groups and the [Cu$_2$(L2)] fragments form 1D ribbons which are linked together into a 2D network through bridging isonicotinate anions, Fig. 13c.

4.3 Other examples

While many examples of d- and f-block coordination polymers of CTV-type ligands with differential guest-binding space fall into the categories discussed in sections 4.1 and 4.2, there are a number of materials with other structural classifications. These include double-bridged chain structures, 2D networks with wave-like rather than two-tiered structures, and some 3-connected 3D frameworks, Table 2. The complex [Ag$_2$(L2)

(DMF)$_2$]·2(BF$_4$)·2(H$_2$O) is another example of a **kgd** network. In this example the hexapodal L2 acts as the 6-connecting centre and the Ag(I) as a trigonal centre.[21] It does not have the tubular structure shown for the previously discussed **kgd** material [Zn(L17)$_2$]$^{2+}$,[17] Fig. 13b, but rather the 2D network has a wave-like aspect. These pack together in the lattice through face-to-face π–π stacking interactions in such a manner that there are both accessible lattice and CTV guest sites, Fig. 14a. Another example of a material with a 2D network and substantial channels is found in [Cu$_5$(L19)$_2$Cl$_{10}$(NMP)$_4$]·n(NMP), which has a decorated **hcb** network topology.[17] There are both mononuclear and dimeric Cu(II)-bridges and NMP-guests are located in both intracavity and lattice sites, Fig. 14b. Both [Cd$_2$(L9)$_2$(NO$_3$)$_4$(NMP)]·9(NMP)·4(H$_2$O) and [Co(L9)(H$_2$O)$_2$]·2(NO$_3$)·2(DMF) have 3,4-connected 2D networks, but the channel sizes are significantly smaller due to 4-fold interpenetration.[16] There are fewer examples involving 3D
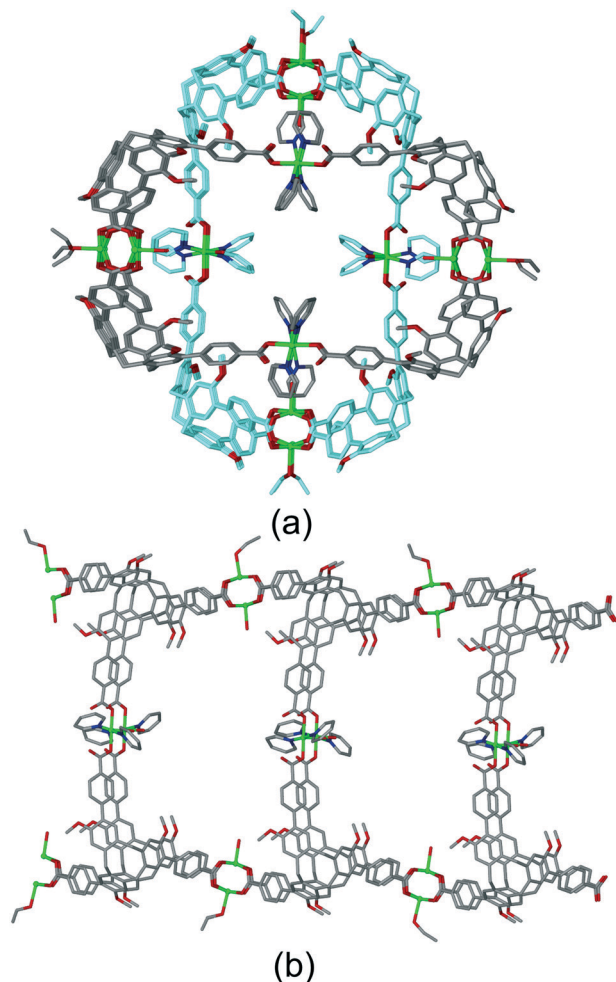
Fig. 12 Structure of [Cu₃(L20)₂(EtOH)(PY)₂(H₂O)₂]. (a) Two interpenetrating tubular 1D coordination polymers. (b) Side-view of one tubular coordination polymer. Disorder sites of terminal ligands not shown for clarity.[23]

coordination networks, the most significant is [Cu₂(L1)₂(NMP)(H₂O)]·4BF₄·12(NMP)·1.5(H₂O). The [Cu₂(L1)₂(NMP)(H₂O)]⁴⁺ network has the **ths** or (10,3)-*b* topology and despite two-fold interpenetration has substantial voids, Fig. 14c.[20]

5. Applications

Thus far, reports of applications of these materials are limited. Guest exchange or guest uptake has been established in some cases, and includes inclusion of small solvent molecules,[26] iodine,[21] and larger fullerene guests.[20] The latter two examples both involved materials whose structures were 2D networks of capsules – [{Re(CO)Br}₃(L2)₂] which binds iodine;[21] and [Cu₃(L3)₄(H₂O)₃]·6(OTf)·*n*(DMSO) which takes up C₆₀,[20] both by immersion in a toluene solution of the guest. Ma has reported the luminescence behaviour of lanthanide-based materials and has shown that they have selective turn-off sensor functionality.[25] Both [Tb(L22)(DMF)₂] and [Eu(L22)(DMF)₂] showed strong luminescence quenching responses, and were selective for: (i) Fe(III) over common 1st

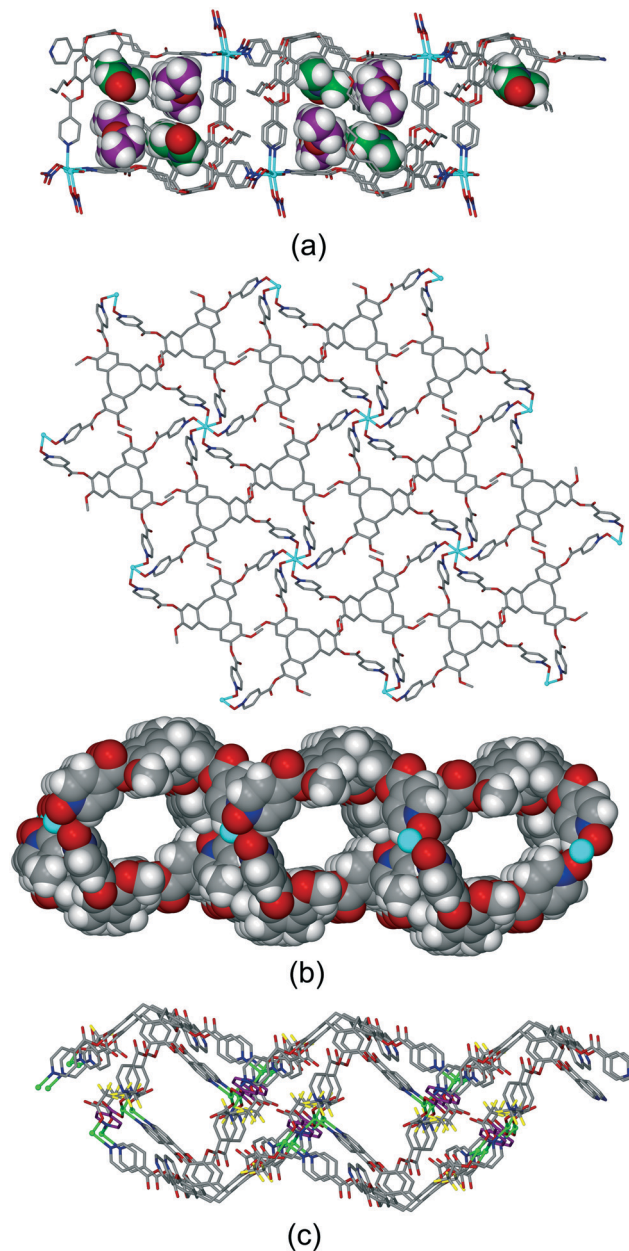**Fig. 13** Examples of two-tiered 2D coordination polymers with tubular channels. (a) [Cd(L1p)(NO₃)₂(H₂O)] with DMF (green) and diethylether (purple) guests shown in distinct pore spaces (some disorder not shown);[19] (b) the **kgd** net of [Zn(L17)₂]²⁺ shown from above and space-fill view down one type of channel;[17] (c) heteroleptic [Cu₂(L2)(TFA)₃(INIC)], with INIC in purple.[21]

row M(II) transition metals, Ag(I) and Na(I); (ii) MnO₄⁻ over a range of anions including Cl⁻ and SO₄²⁻; (iii) nitromethane over other polar solvents including alcohols, acetonitrile and DMF. In terms of detection limits of Fe(III) or MnO₄⁻ in aqueous solution, they performed similarly to or better than other lanthanide CPs. Significantly, these sensor materials appear stable in water with no evidence of hydrolysis of the Ln-carboxylate bonds nor break-down of structure. Ma's heteroleptic [Cd₃(L15)(BDC)₃]·DMF·6H₂O undergoes single-crystal-to-single crystal solvent-exchange with cyclohexane
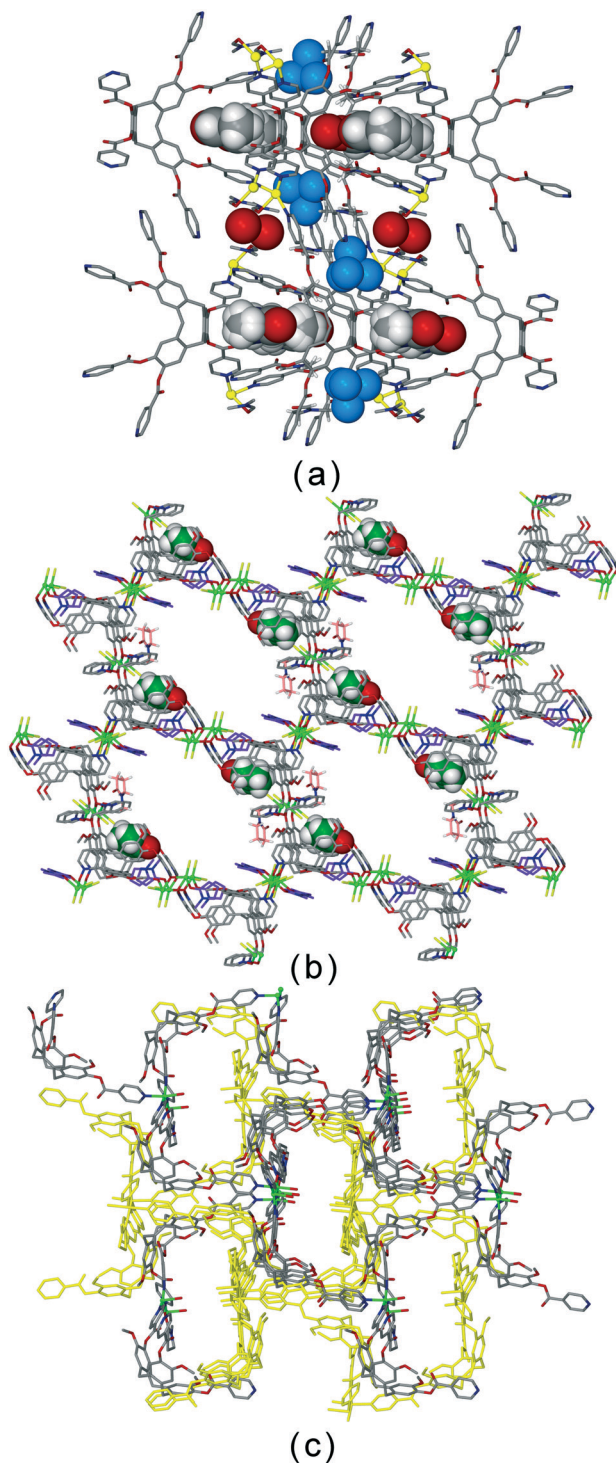
Fig. 14 Examples of other coordination polymers with different types of guest-accessible spaces. (a) [Ag$_2$(L2)(DMF)$_2$]·2(BF$_4$)·2(H$_2$O) packing with guests shown in space-fill;[21] (b) two stacked networks of [Cu$_5$(L19)$_2$Cl$_{10}$(NMP)$_4$]·n(NMP) with intracavity NMP in space-fill, coordinated NMP in purple and lattice NMP in pale pink;[17] (c) [Cu$_2$(L1)$_2$(NMP)(H$_2$O)]·4(BF$_4$)·12(NMP)·1.5(H$_2$O) with one of two interpenetrating networks in yellow and all guest solvent and anions not shown.[20]

with complete exchange of solvent to an isomorphic structure.[25] The parent, the solvent exchanged material and

an isostructural Zn(II) analogue each catalyse the Knoevenagel condensation of benzaldehyde with malononitrile at higher yields than achieved with Cd(NO$_3$)$_2$·4H$_2$O as catalyst. The catalysis was successful for range of benzaldehyde derivatives. Furthermore, both the parent Cd(II) and Zn(II) CPs are efficient co-catalysts with n-Bu$_4$NBr for the cycloaddition of CO$_2$ to a variety of epoxides.[25] These CTV-type ligand CPs were stable catalysts that could be recycled and performed better than other MOF materials for these reactions, with comparable or higher yields over shorter reactions times.

6. Conclusions and outlook

Appending ligands groups to a tribenzo[a,d,g]cyclononatriene core creates tripodal or hexapodal ligands capable of forming a plethora of coordination polymer types when combined with d- or f-block metals. The CPs thus formed show a range of network topologies and the structural outcome of such self-assemblies are not generally predictable. 2D networks are more commonly formed than 3D networks, though examples of the latter do exist. CTV-based ligands are molecular hosts capable of host–guest interactions and self-inclusion motifs. The common inclusion motifs – intracavity guest binding, bowl-in-bowl stacking and the hand-shake self-inclusion – are all observed in different coordination polymers of CTV-type ligands. The latter two motifs, in particular, effectively block the CTV-site, so that CPs with differentiated or hierarchical guest-binding sites are not formed. Some of these observations are highly relevant to CPs constructed from other host molecules. The hand-shake self-inclusion motif is also known for other types of cone-shaped molecules including other classes of tripodal ligand,[40] calixarenes[41] and resorcinarenes.[42] The hand-shake motif has been observed between coordination chains with calixarene-based ligands.[43] Coordinated terminal ligands acting as guests is another blocking motif observed for CTV-based CPs that finds direct parallels with the behaviour of CPs built from other types of cone-shaped macrocyclic hosts.[44]

Coordination polymers of CTV-based ligands which feature differentiated CTV and lattice guest-binding sites most commonly occur where coordination capsule, cage, or cage-like assemblies are linked into 2D or 3D networks. There are a number of examples of 2D networks of capsules in **hcb** or **hxl** topologies. The rational design of such networks with CTV-type ligands remains a challenge. Networked coordination capsules have been reported with other cone-shaped host ligands,[6] and networks of larger coordination cages with pyrogallol[4]arene ligands,[7] so this is a strategy that can be pursued for many different systems. The story is by no means complete, but another emergent trend is that most examples of CTV-ligand CPs with different guest binding sites feature ligands with shorter side-arms. Using ligands with longer side-arms such as L7–L12 promotes interpenetrated structures, which can occur with concomitant inter- or intra-network host–guest interactions such as π–π

stacking hand-shake motif, or guest-binding of terminal ligands. There are currently too few examples to draw trends, however, it is notable that known CPs with hexapodal ligands, and heteroleptic CPs with an additional class of bridging ligand form materials with the desired hierarchical guest-binding spaces. It is relatively straightforward to append ligand-functionality to the CTG and CTC frameworks to give tripodal or hexapodal ligands respectively, hence there is considerable scope for a large array of CPs to be developed, encompassing a variety of ligand functionality and metal types. A number of known such material have been shown to be amenable to guest-exchange or uptake which is a key attribute for development of function in MOFs/CPs. The stability and sensor or catalysis properties demonstrated by Ma's examples, also augers well for the further development of CTV-type coordination polymers as a significant sub-class of networked materials.

Conflicts of interest

There are no conflicts to declare.

Acknowledgements

References

1 Examples of reviews: D. J. Tranchemontagne, J. L. Mendoza-Cortes, M. O'Keeffe and O. M. Yaghi, *Chem. Soc. Rev.*, 2009, **38**, 1257–1283; J. J. Perry, J. A. Perman and M. J. Zaworotko, *Chem. Soc. Rev.*, 2009, **38**, 1400–1417; S. Kitagawa, R. Kitaura and S. Noro, *Angew. Chem., Int. Ed.*, 2004, **43**, 2334–2375; R. Robson, *J. Chem. Soc., Dalton Trans.*, 2000, 3735–3744.

2 Recent reviews: G. Chakraborty, I.-H. Park, R. Medishetty and J. J. Vittal, *Chem. Rev.*, 2021, **121**, 3751–3891; Z. Liang, T. Qiu, S. Gao, R. Zhong and R. Zou, *Adv. Energy Mater.*, 2021, DOI: 10.1002/aenm.202003410; S. Mukherjee, D. Sensharma, O. T. Qazvini, S. Dutta, L. K. Macreadie, S. K. Ghosh and R. Babarao, *Coord. Chem. Rev.*, 2021, **437**, 213852; K.-G. Liu, Z. Sharifzadeh, F. Rouhani, M. Ghorbanloo and M. Ali, *Coord. Chem. Rev.*, 2021, **436**, 213827; J. Liu, J. Huang, L. Zhang and J. Lei, *Chem. Soc. Rev.*, 2021, **50**, 1188–1218; T. A. Goetjen, J. Liu, Y. Wu, J. Sui, X. Zhang, J. T. Hupp and O. M. Farha, *Chem. Commun.*, 2020, **56**, 10409–10418; C.-S. Liu, J. Li and H. Pang, *Coord. Chem. Rev.*, 2020, **410**, 213222; B. M. Connolly, D. G. Madden, A. E. H. Wheatley and D. Fairen-Jimenez, *J. Am. Chem. Soc.*, 2020, **142**, 8541–8549.

3 M. Hoshino, A. Khutia, H. Xing, Y. Inokuma and M. Fujita, *IUCrJ*, 2016, **3**, 139–151; Y. Inokuma, S. Yoshioka, J. Ariyoshi, T. Arai, Y. Hitora, K. Takada, S. Matsunaga, K. Rissanen and M. Fujita, *Nature*, 2013, **495**, 461.

4 S. P. Bew, A. D. Burrows, T. Düren, M. F. Mahon, P. Z. Moghadam, V. M. Sebestyen and S. Thurston, *Chem. Commun.*, 2012, **48**, 4824–4826.

5 Reviews: I. Roy and J. F. Stoddart, *Acc. Chem. Res.*, 2021, **54**, 1440–1453; S. Tashiro and M. Shionoya, *Acc. Chem. Res.*, 2020, **53**, 632–643; A. Ovsyannikov, S. Solovieva, I. Antipin and S. Ferlay, *Coord. Chem. Rev.*, 2017, **352**, 151–186; R. Pinalli, E. Dalcanale, F. Ugozzoli and C. Massera, *CrystEngComm*, 2016, **18**, 5788–5802; H. Zhang, R. Zou and Y. Zhao, *Coord. Chem. Rev.*, 2015, **292**, 74–90; S. Tashiro and M. Shionoya, *Bull. Chem. Soc. Jpn.*, 2014, **87**, 643–654.

6 Y.-J. Hu, J. Yang, Y.-Y. Liu, S. Song and J.-F. Ma, *Cryst. Growth Des.*, 2015, **15**, 3822–3831; A. V. Mossine, C. M. Mayhan, D. A. Fowler, S. J. Teat, C. A. Deakyne and J. L. Atwood, *Chem. Sci.*, 2014, **5**, 2297–2303; H. Tan, S. Du, Y. Bi and W. Liao, *Chem. Commun.*, 2013, **49**, 8211–8213; D. A. Fowler, A. V. Mossine, C. M. Beavers, S. J. Teat, S. J. Dalgarno and J. L. Atwood, *J. Am. Chem. Soc.*, 2011, **133**, 11069–11071.

7 X. Hu, S. Feng, J. Du, L. Shao, J. Lang, C. Zhang, S. P. Kelley, J. Lin, S. J. Dalgarno, D. A. Atwood and J. L. Atwood, *Chem. Sci.*, 2020, **11**, 12547–12552; L. Shao, B. Hua, X. Hu, D. Stalla, S. P. Kelly and J. L. Atwood, *J. Am. Chem. Soc.*, 2020, **142**(16), 7270–7275; C. Zhang, R. S. Patil, C. Liu, C. L. Barnes and J. L. Atwood, *J. Am. Chem. Soc.*, 2017, **139**, 2920–2923.

8 Selected recent examples: H. Ju, J. Y. Lee and S. S. Lee, *CrystEngComm*, 2020, **22**, 7617–7622; X.-X. Wany, J. Yang, X. Xu and J.-F. Ma, *Chem. – Eur. J.*, 2019, **25**, 16660–16667; M. Schulz, A. Gehl, J. Schelnkrich, H. A. Schulze, S. Zimmerman and A. Schaate, *Angew. Chem., Int. Ed.*, 2018, **57**, 12961–12965; X. Hang, B. Liu, S. Wang, Y. Liu and W. Liao, *Dalton Trans.*, 2018, **47**, 1782–1785; B.-B. Lu, W. Jiang, J. Yang, Y.-Y. Liu and J.-F. Ma, *ACS Appl. Mater. Interfaces*, 2017, **9**, 39441–39449; D. M. Miller-Shakesby, B. P. Burke, S. Nigam, G. J. Stasiuk, T. J. Prior, S. J. Archibald and C. Redshaw, *CrystEngComm*, 2016, **18**, 4977–4987.

9 M. J. Hardie and C. J. Sumby, *Inorg. Chem.*, 2004, **43**, 6872–6874.

10 C. J. Sumby and M. J. Hardie, *Cryst. Growth Des.*, 2005, **5**, 1321–1324.

11 C. J. Sumby, J. Fisher, T. J. Prior and M. J. Hardie, *Chem. – Eur. J.*, 2006, **12**, 2945–2959.

12 C. Carruthers, T. K. Ronson, C. J. Sumby, A. Westcott, L. P. Harding, T. J. Prior, P. Rizkallah and M. J. Hardie, *Chem. – Eur. J.*, 2008, **14**, 10286–10296.

13 T. K. Ronson and M. J. Hardie, *CrystEngComm*, 2008, **10**, 1731–1734.

14 C. Carruthers, J. Fisher, L. P. Harding and M. J. Hardie, *Dalton Trans.*, 2010, **39**, 355–357.

15 M. A. Little, M. A. Halcrow, L. P. Harding and M. J. Hardie, *Inorg. Chem.*, 2010, **49**, 9486–9496.

16 M. A. Little, T. K. Ronson and M. J. Hardie, *Dalton Trans.*, 2011, **40**, 12217–12227.

17 J. J. Henkelis, S. A. Barnett, L. P. Harding and M. J. Hardie, *Inorg. Chem.*, 2012, **51**, 10657–10674.

18 J. J. Henkelis, T. K. Ronson and M. J. Hardie, *CrystEngComm*, 2014, **16**, 3688–3693.

19 J. J. Henkelis and M. J. Hardie, *CrystEngComm*, 2014, **16**, 8138–8146.

20 F. L. Thorp-Greenwood, T. K. Ronson and M. J. Hardie, *Chem. Sci.*, 2015, **6**, 5779–5792.

21 F. L. Thorp-Greenwood, G. T. Berry, S. S. Boyadjieva, S. Oldknow and M. J. Hardie, *CrystEngComm*, 2018, **20**, 3960–3970.

22 B. F. Abrahams, N. J. FitzGerald and R. Robson, *Angew. Chem., Int. Ed.*, 2010, **49**, 2896–2899.

23 J.-T. Yu, J. Sun, Z.-T. Huang and Q.-Y. Zheng, *CrystEngComm*, 2012, **14**, 112–115.

24 A. D. Martin, T. L. Easun, S. P. Argent, W. Lewis, A. J. Blake and M. Schröder, *CrystEngComm*, 2017, **19**, 603–607.

25 L. Ma, Q. Zhang, H. Wu, J. Yang, Y.-Y. Liu and J.-F. Ma, *Eur. J. Inorg. Chem.*, 2017, 4221–4230.

26 D.-W. Kang, X. Han, X.-J. Ma, Y.-Y. Liu and J.-F. Ma, *Dalton Trans.*, 2018, **47**, 16197–16204.

27 M. J. Hardie, *Coord. Chem. Rev.*, 2010, **39**, 516–527; A. Collet, *Tetrahedron*, 1987, **43**, 5725–5759.

28 For example: S. Tashiro, S. Hashida and M. Shionoya, *Chem. – Asian J.*, 2012, **18**, 1180–1184; R. Ahmad, A. Franken, J. D. Kennedy and M. J. Hardie, *Chem. – Eur. J.*, 2004, **10**, 2190–2198; D. V. Konarev, S. S. Khasanov, I. I. Vorontsov, G. Saito, M. Yu. Antipin, A. Otsuka and R. N. Lyubovskaya, *Chem. Commun.*, 2002, 2548–2549; M. J. Hardie and C. L. Raston, *Angew. Chem., Int. Ed.*, 2000, **39**, 3835–3839.

29 M. O'Keeffe, M. A. Peskov, S. J. Ramsden and O. M. Yaghi, *Acc. Chem. Res.*, 2008, **41**, 1782–1789.

30 T. K. Ronson, C. Carruthers, J. Fisher, T. Brotin, L. P. Harding, P. J. Rizkallah and M. J. Hardie, *Inorg. Chem.*, 2010, **49**, 675–685.

31 J. L. Scott, D. R. MacFarlane, C. L. Raston and C. M. Teoh, *Green Chem.*, 2000, **2**, 123–126.

32 A. Schaly, M. Meyer, J.-C. Chambron, M. Jean, N. Vanthuyne, E. Aubert, E. Espinosa, N. Zorn and E. Leize-Wanger, *Eur. J. Inorg. Chem.*, 2019, 2691–2706; S. Oldknow, D. Rota Martir, V. E. Pritchard, M. A. Blitz, C. W. G. Fishwick, E. Zysman-Colman and M. J. Hardie, *Chem. Sci.*, 2018, **9**, 8150–8159; V. E. Pritchard, D. Rota Martir, S. Oldknow, S. Kai, S. Hiraoka, N. J. Cookson, E. Zysman-Colman and M. J. Hardie, *Chem. – Eur. J.*, 2017, **23**, 6290–6294; N. J. Cookson, J. M. Fowler, D. P. Martin, J. Fisher, J. J. Henkelis, T. K. Ronson, F. L. Thorp-Greenwood, C. E. Willans and M. J. Hardie, *Supramol. Chem.*, 2018, **30**, 255–266; A. Schaly, Y. Rousselin, J.-C. Chambron, E. Aubert and E. Espinosa, *Eur. J. Inorg. Chem.*, 2016, 832–843; M. J. Hardie, *Chem. Lett.*, 2016, **45**, 1336–1346; J. J. Henkelis and M. J. Hardie, *Chem. Commun.*, 2015, **51**, 11929–11943; Z. Zhong, A. Ikeda, S. Shinkai, S. Sakamoto and K. Yamaguchi, *Org. Lett.*, 2001, **3**, 1085–1087.

33 Review T. Brotin and J.-P. Dutasta, *Chem. Rev.*, 2009, **109**, 88–130.

34 Y. Kawakami, T. Ogishima, T. Kawara, S. Yamauchi, K. Okamoto, S. Nikaido, D. Souma, R.-H. Jin and Y. Kabe, *Chem. Commun.*, 2019, **55**, 6066–6069; J. L. Holmes, B. F. Abrahams, A. Ahveninen, B. A. Boughton, T. A. Hudson, R. Robson and D. Thinagaran, *Chem. Commun.*, 2018, **54**, 11877–11880; D. Xu and R. Warmuth, *J. Am. Chem. Soc.*, 2008, **130**, 7520–7521.

35 For example: G. T. Illa, S. Hazra, P. Satha and C. S. Purohit, *CrystEngComm*, 2017, **19**, 4759–4765; E. Huerta, S. A. Serapian, E. Santos, E. Cequier, C. Bo and J. de Mendoza, *Chem. – Eur. J.*, 2016, **22**, 13496–13505; L. Wang, G.-T. Wang, X. Zhao, X.-K. Jiang and Z.-T. Li, *J. Org. Chem.*, 2011, **79**, 3531–3535; S. B. Lee and J.-I. Hong, *Tetrahedron Lett.*, 1996, **37**, 8501–8504.

36 S. T. Mough and K. T. Holman, *Chem. Commun.*, 2008, 1407–1409.

37 J. Su, L. Yao, J. Zhang, S. Yuan, F. Xie, Y. Ding, M. Zhao, S. Wang, H. Li, S. Zhang, J. Wu and Y. Tian, *New J. Chem.*, 2016, **40**, 97–100.

38 T. Grancha, A. Carné-Sánchez, F. Zarekarizi, L. Herández-López, J. Albalad, A. Khobotov, V. Guillerm, A. Morsali, J. Juanhuix, F. Gándara, I. Imaz and D. Maspoch, *Angew. Chem., Int. Ed.*, 2021, **60**, 5729–5733; H.-N. Wang, F.-H. Liu, X.-L. Wang, K.-Z. Shao and Z.-M. Su, *J. Mater. Chem. A*, 2013, **1**, 13060–13063; H.-N. Wang, X. Meng, G.-S. Yang, X.-L. Wang, K.-Z. Shao, Z.-M. Su and C.-G. Wang, *Chem. Commun.*, 2011, **47**, 7128–7130; H. Chun, H. Jung and J. Seo, *Inorg. Chem.*, 2009, **48**, 2043–2047; J.-R. Li, D. J. Timmons and H.-C. Zhou, *J. Am. Chem. Soc.*, 2009, **131**, 6368–6369.

39 For example: A. Legrand, L.-H. Liu, P. Royla, T. Aoyama, G. A. Craig, A. Carné-Sánchez, K. Urayama, J. J. Weigand, C.-H. Lin and S. Furakawa, *J. Am. Chem. Soc.*, 2021, **143**, 3562–3570; C. Lu, M. Zhang, D. Tang, X. Yan, Z. Zhang, Z. Zhou, B. Song, H. Wang, X. Li, S. Yin, H. Sepehrpour and P. J. Stang, *J. Am. Chem. Soc.*, 2018, **140**, 7674–7680.

40 W. Wei, G. Wang, Y. Zhang, F. Jiang, M. Wu and M. Hong, *Chem. – Eur. J.*, 2011, **17**, 2189–2198.

41 For example: M. Makha, C. L. Raston and A. N. Sobolev, *Aust. J. Chem.*, 2006, **59**, 260–262; J. Martz, E. Graf, M. W. Hosseini, A. De Cian and N. Kyritsakas-Gruber, *C. R. Chim.*, 2002, **5**, 481–486; E. B. Brouwer, K. A. Udachin, G. D. Enright, J. A. Ripmeester, K. J. Ooms and P. A. Halchuk, *Chem. Commun.*, 2001, 565–566.

42 S. Ma, D. M. Rudkevich and J. Rebek, *J. Am. Chem. Soc.*, 1998, **120**, 4977–4981.

43 C. Y. Goh, T. Becker, D. H. Brown, B. W. Skelton, F. Jones, M. Mocerino and M. I. Ogden, *Chem. Commun.*, 2011, **47**, 6057–6059.

44 P. P. Cholewa, C. M. Beavers, S. J. Teat and S. J. Dalgarno, *Cryst. Growth Des.*, 2013, **13**, 5165–5168; P. P. Cholewa, C. M. Beavers, S. J. Teat and S. J. Dalgarno, *Chem. Commun.*, 2013, **49**, 3203–3205.